Chemical Science

ROYAL SOCIETY OF CHEMISTRY

EDGE ARTICLE

View Article Online
View Journal

Cite this: DOI: 10.1039/d5sc10093c

All publication charges for this article have been paid for by the Royal Society of Chemistry

Stereospecific alkenylation of carboranes: copper-catalyzed access to pyridylcarboranyl alkenes

Ping Li,†[a] Xiang Li,†[a] Liyan Wang,†[b] Mengmeng Wang,[b] Deshuang Tu,*[b] Hong Yan,*[b] Jian Lu*[c] and Ju-You Lu*[a]

The direct functionalization of carbon vertices in polyhedral carboranes has received considerable attention because of their wide applications in functional materials, catalysis, and pharmaceuticals. However, achieving direct C–H bond activation of *o*-carboranes remains a challenge, as it typically requires strong bases to facilitate the deprotonation of the C–H bonds. Herein, we report a copper-catalyzed stereospecific C–H alkenylation of *o*-carboranes using Na_2CO_3 as a mild base. Remarkably, the reaction exhibits stereospecificity, allowing for switchable *syn*- or *anti*-selectivity simply by employing the *E*- or *Z*-configuration of the alkenyl halide coupling partner. Structurally diverse *E*- and *Z*-alkenylcarboranes are accessible by this protocol, among which the latter are difficult to access by existing methods. The synthetic utility of this methodology was demonstrated by the late-stage modification of amino acids, sugars, and drug molecules. Furthermore, the synthesized carboranylethylene scaffolds exhibit aggregation-induced emission and bright solid-state luminescence, with quantum yields reaching 67%. Thus, this work unveils a Cu(I)/Cu(III) catalytic model for the C–H activation of carboranes and establishes pyridylcarborane–alkene hybrids as a new class of functional, bioisosteric architectures.

Received 24th December 2025
Accepted 3rd February 2026

DOI: 10.1039/d5sc10093c

rsc.li/chemical-science

Introduction

Carboranes, a class of three-dimensional icosahedral boron–carbon clusters, have emerged as unique and valuable building blocks in molecular design.[1–4] Their spherical geometry, high boron content, and three-dimensional σ-aromaticity offer a compelling "escape from flatland," positioning them as superior bioisosteric replacements for two-dimensional arenes in the development of pharmaceuticals, bioactive agents, and advanced materials (Scheme 1A).[5]

Within this paradigm, the arylethylene motif is a ubiquitous and critical framework in functional molecules. It is a cornerstone of structures ranging from aggregation-induced emission (AIE)-active luminogens[6] and phototherapeutic agents[7] to numerous FDA-approved drugs (Scheme 1A).[8] Inspired by this prevalence, we recognized a great opportunity: the development of carborane-based mimetics of these valuable arylethylene systems. Such a replacement, analogous to a carborane-based analogue of tamoxifen, holds immense promise for creating novel boron-cluster-functionalized molecules with tailored properties.[9] Consequently, over the past decades, tremendous efforts have been made for the development of carborane C-alkenylation strategies, including condensation reactions,[10a] Ullmann-type coupling,[10b] coupling of metal–carboryne complexes,[10c] Wittig reactions,[10d] and photo-induced reactions.[10e,f] However, synthetic access to such carbon-substituted *o*-carborane architectures is limited, and stereochemical control represents a significant hurdle.[10,11] In particular, a general and stereospecific route to *Z*-configured carboranylethylenes has been especially elusive (Scheme 1B).

To overcome this limitation, here we conceived a strategy based on a stereospecific reaction. Namely, the stereochemical information encoded in readily available *Z*/*E*-arylethylenes could be transferred[12] through a catalytic cycle to dictate the geometry of the final carboranylethylene products (Scheme 1C). This approach would enable precise stereocontrol, a critical factor for function in both biological and materials contexts. Herein, we report the realization of this strategy through a copper-catalyzed stereospecific C–H alkenylation of *o*-carboranes. This method provides efficient access to a diverse range of pyridylcarboranyl alkenes with high fidelity in stereochemical transfer. The resulting C-alkenylcarborane scaffolds serve as versatile building blocks, which we have leveraged to construct AIE-active luminogens with bright and tunable emission and to develop novel drug candidates, thereby demonstrating their significant potential in both materials science and medicinal chemistry.

[a]*School of Chemistry and Chemical Engineering, Hainan University, Haikou, 570228, China. E-mail: lujy@hainanu.edu.cn*

[b]*State Key Laboratory of Coordination Chemistry, School of Chemistry and Chemical Engineering, Nanjing University, Nanjing, 210023, China. E-mail: tudeshuang@nju.edu.cn; hyan1965@nju.edu.cn*

[c]*State Key Laboratory of Fluorine & Nitrogen Chemicals, Xi'an Modern Chemistry Research Institute, Xi'an, 710065, China. E-mail: lujian204@263.net*

† P. L., X. L. and L. W. contributed equally.

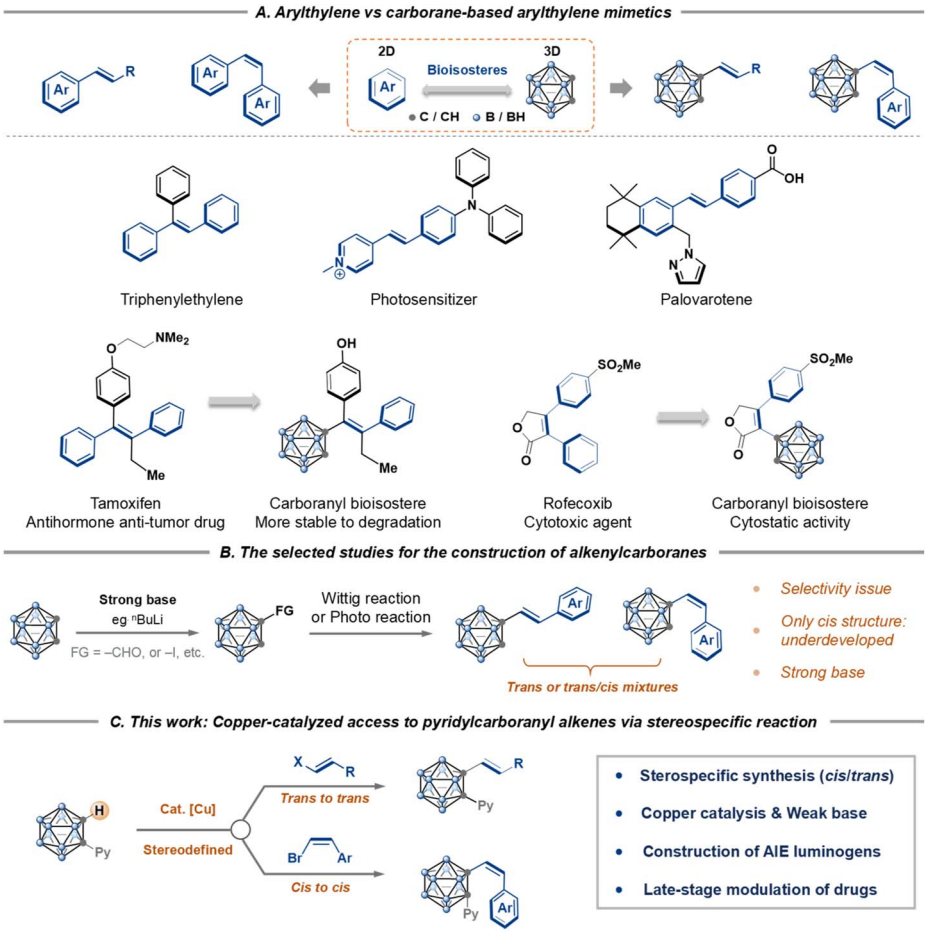

Scheme 1 Outline of this work.

Results and discussion

Initially, we investigated the C–H alkenylation of 1-(pyridin-2-yl)-*o*-carborane (**1a**) with (*E*)-1-(2-bromovinyl)naphthalene (**2l**) in the presence of various copper catalysts. After many attempts (see the SI for details), gratifyingly, with the use of a catalytic amount of $Cu(acac)_2$, the cage C–H alkenylation provided the desired C-alkenylcarborane **3l** in a 90% isolated yield.

Next, we evaluated the substrate scope of the copper-catalyzed stereospecific C–H alkenylation of *o*-carboranes with vinyl electrophilics (Scheme 2). First, we tested various vinyl halides bearing diverse functional groups. The reaction of *E*-bromostyrene afforded alkenylcarborane **3a** with exclusive retention of the configuration, indicating that a stereospecific process occurs. Several vinyl halides were compatible, including inert chlorides and reactive bromides. The former is a challenging substrate for conventional coupling reactions. Various aryl-conjugated β-vinyl halides possessing electron-donating (**3b–3g**) and electron-withdrawing (**3h**, and **3i**) groups were tested, affording the desired products with excellent *anti*-selectivity and high yields. A wide variety of functional groups are tolerated, including valuable handles for further functionalization: aryl bromides, esters, and free hydroxyl groups. The cage C–H coupling was not limited to heterocyclic compounds, including thiophene (**3j**) and furan (**3k**). Naphthyl-conjugated vinyl bromide afforded **3l** in 90% yield. In contrast, the conversion rate was significantly improved, and no *syn*-isomer product was detected,[10e] thereby greatly simplifying product isolation. Notably, polysubstituted olefins such as 1,1-diphenyl (**3m**) and 1,1,2-triphenyl (**3n**) scaffolds were well tolerated, providing boron cluster-based AIE-active luminogens (AIEgens, *vide infra*). Other vinyl electrophiles were coupled effectively, including sterically hindered α-bromostyrene (**3o**), 2-bromoindene (**3p**), and (4-bromo-1,3-butadien-1-yl)benzene (**3q**). In the previous report, substrates possessing aliphatic vinyl resulted in β′-H elimination to form a mixture of "Heck-type" and "ene-reaction-type" products.[10c] Here, several aliphatic bromoalkenes were exclusively converted to alkenylcarboranes (**3r–3u**). To investigate the robustness of this method, we also examined a mixture of *Z*- and *E*-haloalkenes, which we envisioned could perturb the *Z*/*E*-selectivity by competitive reactions. Notably, the maintenance of the *Z* : *E* ratio of products **3s** and **3t** further confirmed that the cage C–H alkenylation is a highly stereoselective process. Esters and amides conjugated with a double bond were viable for this protocol (**3v–3z**), among which amides are widely used as directing groups for C–H activation in organic synthesis.

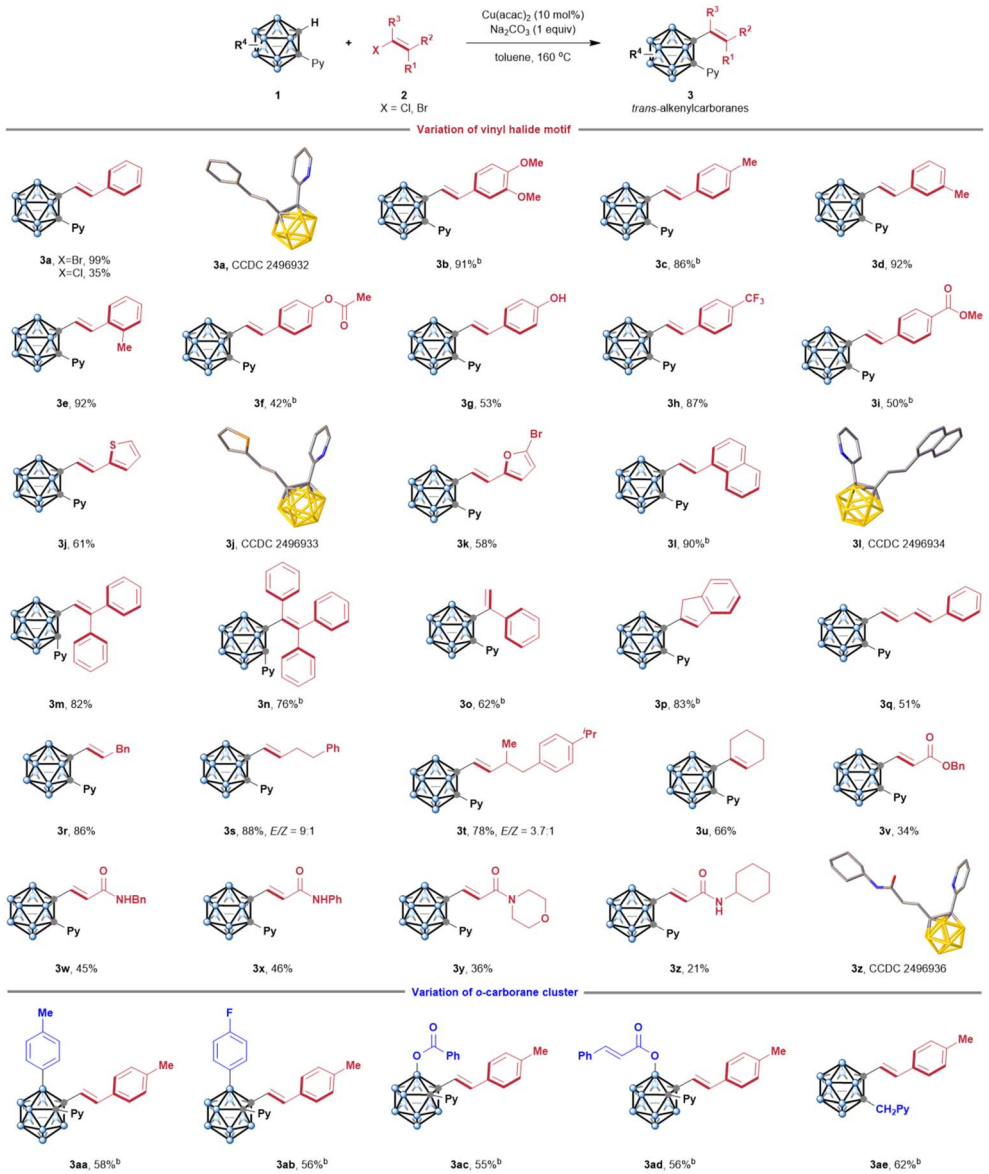

Scheme 2 Substrate scope for the *E*-alkenylation of *o*-carboranes[a]. [a]Conditions: **1** (0.1 mmol), **2** (3.0 equiv.), $Cu(acac)_2$ (10 mol%), Na_2CO_3 (1.0 equiv.), toluene (1.0 mL), 160 °C, 12 h. Isolated yield. [b]**2** (1.5 equiv.) was used. The hydrogen atoms of crystal structures are omitted for clarity.

Next, we evaluated substituted *o*-carboranes. Various B(3)-substituted *o*-carboranes were compatible with this protocol. Sterically hindered B(3)-aryl carboranes bearing electron-donating (**3aa**) and electron-withdrawing (**3ab**) groups on the phenyl group all gave gratifying outcomes. Acyl-protected B(3)-hydroxyl *o*-carboranes worked well to provide the target products **3ac** and **3ad**, respectively. Additionally, picolyl group-directed cage C–H alkenylation was also achieved using copper catalysis (**3ae**). The reaction of 1-Ph-*o*-carborane (**1f**) or unsubstituted *o*-carborane (**1g**) and *trans*-β-bromostyrene (**2a**) did not proceed as the starting materials were fully recovered (Scheme S6). These results revealed that the pyridyl group, which acts as a directing group to facilitate the activation of C–H bonds, is essential and also provides a versatile platform for expanding the chemical space of boron cluster-based structural diversity.

Encouraged by these results, we extended this method to bromoalkenes with a more challenging *Z* configuration (Scheme 3). It should be noted that modular synthesis of *Z*-alkenylcarborane through various methods has been a long-standing challenge. Using the Wittig reaction of C-formyl-*o*-carborane with a triphenyl phosphonium ylide produced alkenylcarborane as a 6 : 4 mixture of *E*/*Z* isomers.[10f] The photo-alkenylation of iodocarborane with 2-vinylnaphthalene gave the alkenylated product in 22% yield with a 5.3 : 1 *E* : *Z* ratio.[10e] Nevertheless, these early studies prompted us to investigate whether this copper catalysis can achieve *syn*-selective alkenylation by cage C–H activation. Gratifyingly, employing (*Z*)-β-bromostyrene as a coupling partner exclusively afforded the desired *syn*-alkenylation product **5a** with excellent yield. A diverse range of *Z*-bromoalkenes, featuring substituents at different positions on the phenyl ring, were generally well

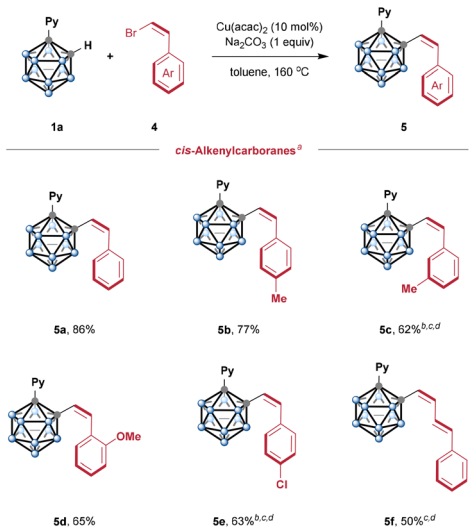

Scheme 3 Substrate scope for the *Z*-alkenylation of *o*-carboranes[a]. [a]Conditions: **1a** (0.1 mmol), **4** (3.0 equiv.), $Cu(acac)_2$ (10 mol%), Na_2CO_3 (1.0 equiv.), toluene (1 mL), 160 °C, 12 h. Isolated yield. [b]**4** (4.0 equiv.). [c]$Cu(acac)_2$ (20 mol%). [d]24 h.

tolerated, affording *Z*-alkenylcarboranes (**5b–5e**) with excellent *syn*-selectivity and good yields. Additionally, the 1,3-dienyl substrate was also competent in this *syn*-selective process (**5f**).

To probe the inherent selectivity in the competitive coupling of vinyl and aryl electrophiles, we further investigated the carboranylation of various electrophiles (Scheme 4). The Cu catalysis offers a selectivity that is complementary to those achieved by conventional coupling protocols. For example, our group has recently reported the C–H arylation of *o*-carborane with aryl electrophiles.[13] Here, under Cu catalysis, employing electrophiles containing a vinyl bromide and an aryl electrophile, including the fluoride (**3af**), chloride (**3ag**), and even

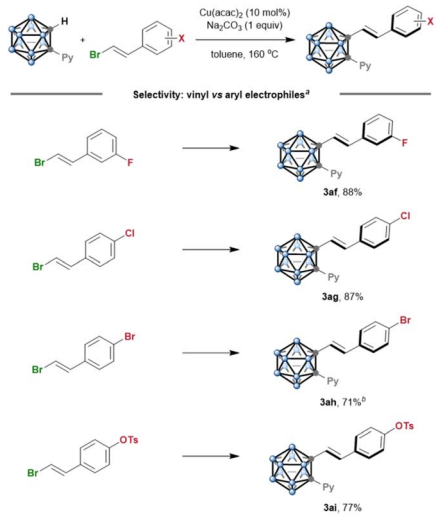

Scheme 4 Chemoselective cage C-alkenylation with various electrophiles[a]. [a]Conditions: **1a** (0.1 mmol), **2** (1.5 equiv.), $Cu(acac)_2$ (10 mol%), Na_2CO_3 (1.0 equiv.), toluene (1.0 mL), 160 °C, 12 h. Isolated yield. [b]**2** (3.0 equiv.) was used.

highly reactive bromide (**3k** and **3ah**) and tosylate (**3ai**), provides completely exclusive selectivity for the C-alkenylated products.

Given the fact that the current protocol offers a powerful reaction platform for the C–H alkenylation of *o*-carboranes, its synthetic applications were further investigated. First, carborane-containing ferrocenes are widely used in composite solid propellants due to their ability to regulate the burning rate.[14] We were pleased to observe that a ferrocene-derived bromoalkene was successfully incorporated with *o*-carborane (**7a**) (Scheme 5A). Moreover, to underscore the utility of the cage C–H alkenylation for drug-discovery purposes, we examined a range of active pharmaceutical ingredients (Scheme 5B). Vinyl bromides bearing bioactive structures such as mefenamic acid (**7b**), ketoprofen (**7c**), flurbiprofen (**7d**), probenecid (**7e**), indometacin (**7f**), and aspirin (**7g**) were coupled to *o*-carborane in good to excellent yields. The compatibility of unprotected amines (**7b**) with the reaction conditions is noteworthy for medicinal chemistry, considering the ubiquity of this functionality among lead compounds.

The combination of carboranes and amino acid or glycoside fragments in one structure can serve as a basis for obtaining promising targeted boron delivery agents for cancer treatment by boron neutron capture therapy (BNCT).[5] L-Alanine-derived bromoalkene could be readily converted to a boronated amino acid (**7h**). Moreover, mannofuranose- and D-glucopyranose-containing bromoalkenes delivered boron clusters conjugated with glycosides (**7i** and **7j**). The amenability of this new chemistry to complex drug molecules demonstrates the potential of this transformation to achieve late-stage diversification in pharmaceutically relevant settings (Scheme 5C).

To demonstrate the synthetic utility of the reaction, we performed the derivatization of **3ah** (Scheme 5D). The metal-catalyzed cross-coupling toolkit can be employed for the structural elaboration of the aryl bromide group for the cage C-vinylated products. For example, the Suzuki–Miyaura reaction of **3ah** proceeded smoothly, delivering the C–C coupling products **8a** and **8b** in useful to good yields. Specifically, *o*-carborane-containing triphenylamine is expected to be a potential photofunctional molecule.[3] Moreover, to rapidly produce drug-like molecular architecture from native functionality, erlotinib, a popularly used lung cancer-targeting drug, was chosen to combine with **3ah** by the facile Sonogashira reaction; thus, the BNCT drug candidate **8c** could be prepared from *o*-carboranes in two steps.

Finally, successful iterative C–H activation of *o*-carborane was also demonstrated, providing a novel 2-fold C–H-functionalized bis(*o*-carborane) **8d** in good yield (Scheme 5E). The tactical union of two powerful, recently invented transformations for chemical synthesis (catalytic cage C–H alkenylation and arylation) enables access to previously challenging molecular space.[13]

Carboranes have emerged as versatile building blocks for constructing luminescent materials. Herein, we present an efficient synthetic strategy to access hybrid conjugates integrating boron clusters with π-conjugated units. These hybrids are anticipated to exhibit efficient luminescence in the aggregate state, leveraging the synergistic steric bulk and electron-

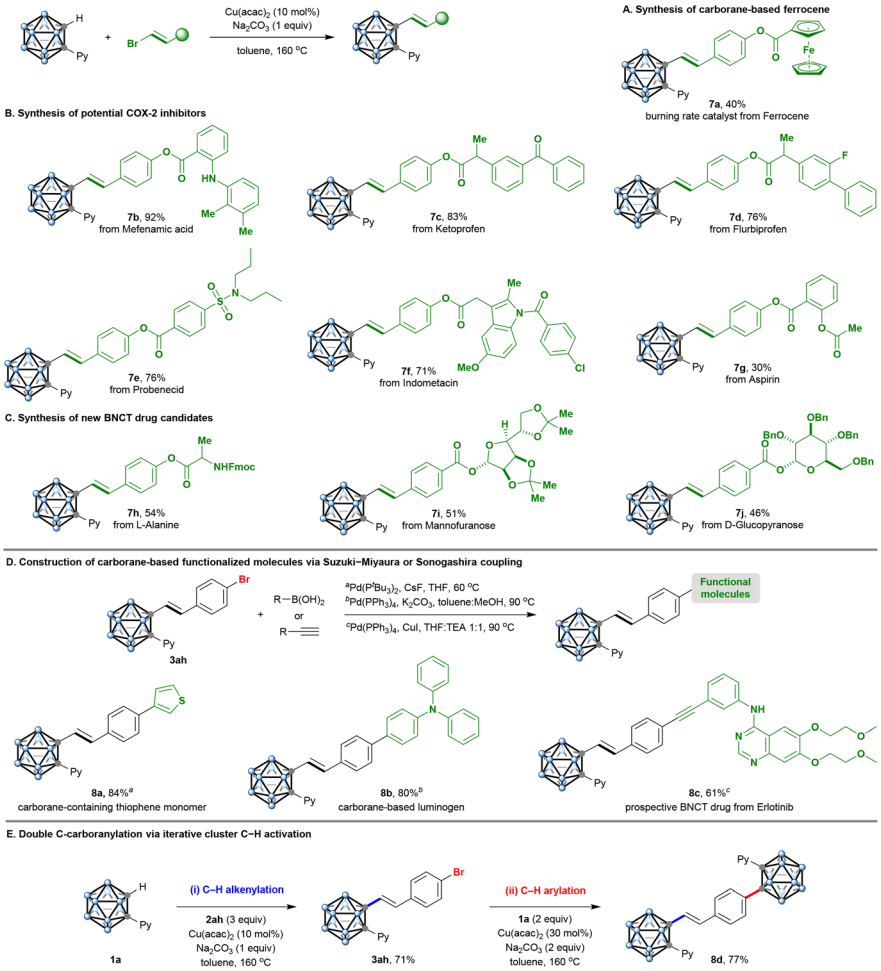

Scheme 5 Synthetic applications.

withdrawing nature of the carborane moiety.[14,15] To validate this hypothesis, compounds **3j**, **3l**, **3n**, and **3q** were selected for photophysical characterization. As anticipated, photoluminescence (PL) studies in mixed solvents revealed pronounced AIE behavior (Fig. 1A and B). For instance, at water fractions below 70%, negligible emission intensity was observed—consistent with typical AIE luminogens. Upon increasing the water fraction beyond this threshold, a dramatic enhancement in PL intensity occurred, confirming AIE characteristics.[16] Analogous behavior was observed for other carborane-based derivatives (Fig. S1–S3). Notably, these compounds exhibit bright, color-tunable emission in the solid state (Fig. 1C) with high absolute quantum yields (ϕ) of up to 67% (Fig. 1D and S4–S7), rivaling classical AIE luminogens such as tetraphenylethene (TPE).[17]

To elucidate the origin of efficient solid-state luminescence, we analyzed single-crystal X-ray structures of **3l** (Fig. 1E). The incorporation of the carborane unit induces a V-shaped molecular geometry, which mitigates π–π stacking interactions between aromatic rings. Instead, multiple intermolecular interactions such as H⋯H and C–H⋯N contacts dominate the crystal packing. This structural motif suppresses the formation of non-emissive exciplex species, rationalizing the observed emission efficiency.[18] Complementary theoretical calculations reveal that the highest occupied molecular orbitals (HOMOs) of these compounds reside predominantly on the arylvinyl moieties, while the lowest unoccupied molecular orbitals (LUMOs) significantly delocalize onto the *o*-carborane unit (Fig. 1F). This electronic separation strongly supports emission originating from charge-transfer (CT) states. Notably, the electronic structure of these carborane-based systems contrasts sharply with their phenyl-substituted counterparts (*e.g.*, 2-styrylthiophene and 1-styrylnaphthalene, Fig. S8). Given the tunable properties imparted by the carborane moiety, these molecular frameworks present compelling opportunities for designing advanced photofunctional materials.

Preliminary mechanistic studies were conducted to gain further insight into the cage C–H alkenylation (Fig. 2A). First, the reaction of 1-(pyridin-2-yl)-*o*-carborane **1a** with *n*-BuLi, followed by the addition of 1.5 equiv. of CuCl, afforded a key cyclometalated copper(I) intermediate (**II**), subsequent reaction with 1-[(1*E*)-2-bromoethenyl]-4-methylbenzene (**2c**) produced the C-alkenylated *o*-carborane **3c** in 90% total yield. Trials to characterize this intermediate through NMR analysis were

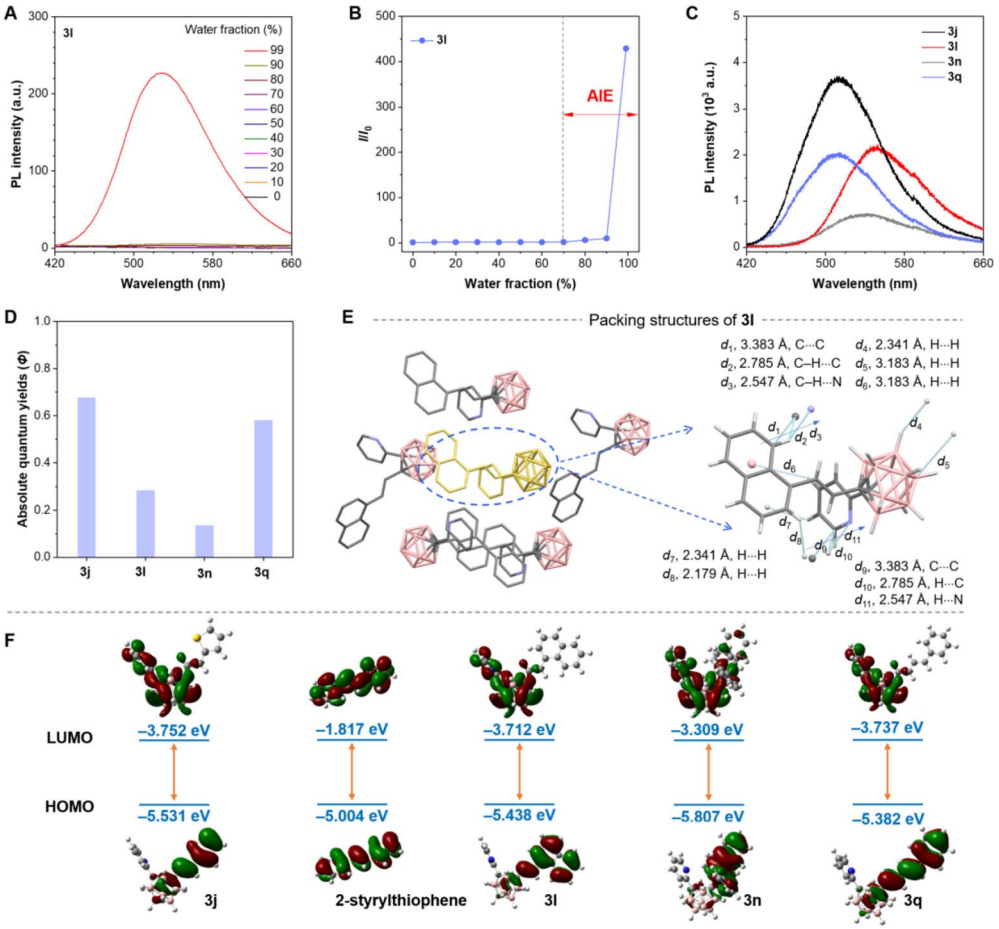

Fig. 1 Photophysical properties and structural analysis of carborane-based luminogens **3j**, **3l**, **3n**, and **3q**. (A) Photoluminescence (PL) spectra of **3l** in THF/H_2O mixture solvents at varied water fractions. (B) Relative PL intensity (I/I_0) for **3l** *versus* water fraction. (C) Solid-state PL spectra of **3j**, **3l**, **3n**, and **3q**. (D) Absolute solid-state photoluminescence quantum yields (ϕ). (E) Crystal packing structures of **3l**. The hydrogen atoms of the crystal structures are omitted for clarity. (F) Computed excited-state HOMO and LUMO isosurface plots for **3j**, 2-styrylthiophene, **3l**, **3n**, and **3q**.

unsuccessful. To our delight, HRMS measurement successfully detected the elusive intermediate (**II**) (Fig. S9). Furthermore, complex (**II**), when subjected to the catalytic conditions with 1.5 equiv. of **2c** as the coupling partner, afforded **3c** in 69% yield as the sole product. Under standard conditions, complex (**II**) catalysed C–H alkenylation efficiently, leading to **3c** with excellent yield. These results indicated that formation of a five-membered cyclometalated complex is a key step in the early stages of the catalytic cycle.

Notably, 2-phenylpyridine did not react with **2a** under the optimal reaction conditions, indicating a significant difference in reactivity between the 3D delocalized σ aromatic *o*-carborane and the 2D aromatic benzene (Scheme S7). On the other hand, competition reactions between *cis*- or *trans*-bromoalkene substrates were performed, affording a mixture of *cis*- and *trans*-pyridylcarboranyl alkenes **5a** and **3a** in 92% yield with a 60 : 40 *Z* : *E* ratio. These results suggest that *cis*-bromoalkenes are more reactive (Scheme S9). In addition, radical capture experiments with TEMPO (2,2,6,6-tetramethylpiperidyl-1-oxyl) were conducted. The reaction proceeded unaffected, thus excluding the radical mechanism (Scheme S11).

To find support for the proposed reaction mechanism, we sought to prepare the hypothesized cyclometalated complex. The isolation and characterization of copper–carborane complexes has been a long-standing challenge, possibly due to their high reactivity or low solubility.[19] In the presence of weak base sodium carbonate, the stoichiometric reaction of **1a** with copper salt did not generate an observable amount of copper species by ^{1}H NMR. Finally, we found that the reaction of **II** in ethyl acetate at room temperature afforded a rare copper(II)-carborane complex (**II'**). The structure of this Cu(II) complex was confirmed by X-ray diffraction. Single-crystal analysis clearly indicated a Cu(II) dinuclear complex with an asymmetric double bridge formed by a μ-carboxylato and a μ-hydroxo ligand, resulting in an exopolyhedral C–Cu bond. The C(2)–Cu distance is 1.978(2) Å, which is consistent with recent reports on the related lithium *o*-carboranyl cuprate complex.[20] The ancillary ligand on each copper center is the non-symmetric C, N chelate 1-pyridylcarboranyl bonded to the metal through a hard-donor nitrogen and a softer σ-bonded carbon atom (Fig. 2B). Surprisingly, complex (**II'**) is the first known identifiable example of copper(II)-*o*-carborane dinuclear complexes

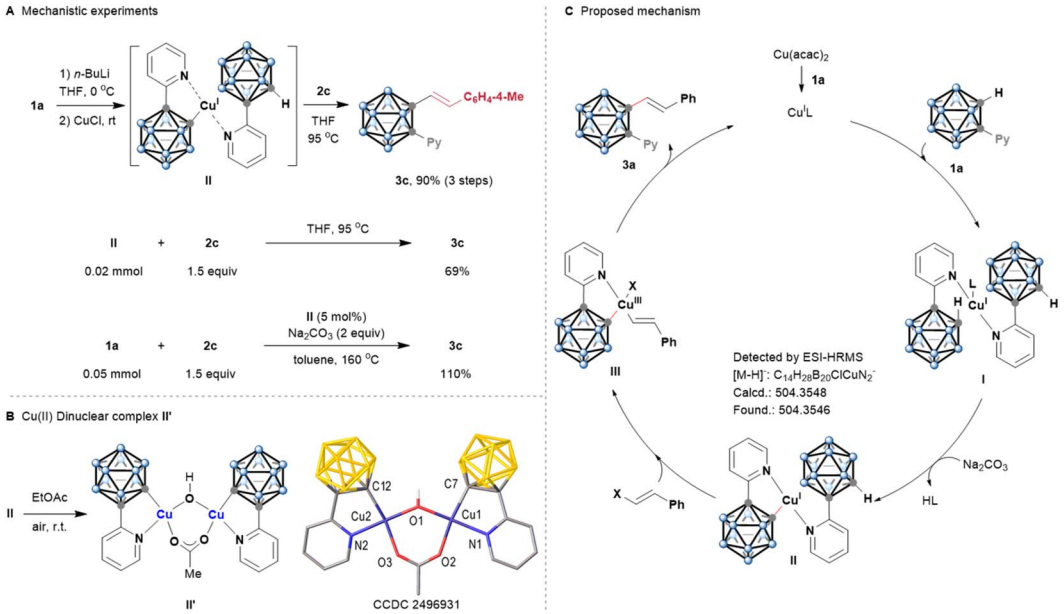

Fig. 2 Mechanistic investigations. (A) Mechanistic experiments. (B) Formation and X-ray crystal structure of dinuclear complex II'. Hydrogen atoms except for O–H are omitted for clarity. Selected bond distances [Å]: Cu2–O1 1.8899(17), Cu2–O3 1.9314(19), Cu2–N2 2.047(2), Cu2–C12 1.971(2). (C) Plausible catalytic cycle.

containing an exopolyhedral C–Cu bond. Unfortunately, this complex is not catalytically active for this reaction.

On the basis of our observations and previous reports,[13] a plausible reaction mechanism is proposed in Fig. 2C. Reduction of Cu(II) by *o*-carborane or a base forms Cu(I) species.[21] A bidentate chelation of **1a** with Cu(I) occurs to give the intermediate (**I**). Subsequently, in the presence of Na_2CO_3, cage C–H bond metalation of **I** generates a key cyclometalated intermediate copper(I)-*o*-carborane complex (**II**). Oxidative addition of Cu(I) by alkenyl halide affords the Cu(III) species (**III**), which undergoes C–C reductive elimination to give products **3a** and regenerate the catalytically active Cu(I) complex. It is noteworthy that the double bond geometry of alkenyl halide reactants was fully retained in all of the stereospecific cage C–H alkenylation products.

Conclusions

In summary, we have developed an efficient Cu-catalyzed direct C–H alkenylation of *o*-carboranes by a stereospecific strategy. The use of easily accessible starting materials, a broad substrate scope, a good functional group tolerance, excellent stereospecific selectivity, mild base Na_2CO_3, and the versatile functionalization of the C-alkenylated *o*-carboranes render this method highly practical and appealing. This has enabled the fast construction of a new library of boron cluster-based functionalized molecules, including carborane-based luminogens and BNCT drug candidates. More importantly, these new boron cluster-based luminogens display interesting properties of enhanced solid-state luminous efficiency and AIE effects. This work offers an efficient method to construct boron cluster-based functional molecules, and may have great potential in biological applications and other related fields.

Author contributions

J.-Y. L., D. T. and H. Y. conceived of the work. J.-Y. L., D. T., H. Y. and J. L. supervised the project. P. L., X. L., L. W. and M. W. ran the experiments. P. L., X. L., L. W., D. T. and J.-Y. L. analyzed the data. J.-Y. L. and D. T. wrote the manuscript. P. L., X. L., D. T. and J.-Y. L. provided revisions.

Conflicts of interest

There are no conflicts to declare.

Data availability

Data supporting this study are available in the supplementary information (SI) and further details are available from the authors on reasonable request. Supplementary information: experimental procedures and data for new compounds. See DOI: https://doi.org/10.1039/d5sc10093c.

CCDC 2496931–2496934 and 2496936 contain the supplementary crystallographic data for this paper.[22a–e]

Acknowledgements

This work was supported by the National Natural Science Foundation of China (22161015) and Hainan Provincial Natural Science Foundation of China (221RC448). This work was also supported by the Fundamental Research Funds for the Central Universities (2024300362), the National Natural Science Foundation of China (92461308, 92261202, W2412072, 22401141 and 22571145) and the Natural Science Foundation of Jiangsu Province (BK20241229). The high-performance computing center of Nanjing University is acknowledged.

Notes and references

1 (*a*) R. N. Grimes, *Carboranes*, Elsevier, Oxford, 3rd edn, 2016, p. 283; (*b*) J. Poater, C. Viñas, I. Bennour, S. Escayola, M. Solà and F. Teixidor, *J. Am. Chem. Soc.*, 2020, **142**, 9396–9407; (*c*) J. Poater, C. Viñas, M. Solà and F. Teixidor, *Nat. Commun.*, 2022, **13**, 3844–3851; (*d*) N. S. Hosmane and R. D. Eagling, *Handbook of Boron Science: With Applications in Organometallics, Catalysis, Materials and Medicine*, World Scientific, London, 2018; (*e*) N. S. Hosmane, *Boron Science: new Technologies and Applications*, CRC Press, 1st edn, 2012, p. 878; (*f*) M. Solà, *Nat. Chem.*, 2022, **14**, 585–590; (*g*) T. L. Chan and Z. Xie, *Chem. Sci.*, 2018, **9**, 2284–2289.

2 (*a*) A. R. Popescu, F. Teixidor and C. Viñas, *Coord. Chem. Rev.*, 2014, **269**, 54–84; (*b*) R. Núñez, M. Tarrés, A. Ferrer-Ugalde, F. F. de Biani and F. Teixidor, *Chem. Rev.*, 2016, **116**, 14307–14378; (*c*) P.-F. Cui, X.-R. Liu and G.-X. Jin, *J. Am. Chem. Soc.*, 2023, **145**, 19440–19457; (*d*) P. Cui, X. Liu, Y. Lin, Z. Li and G. Jin, *J. Am. Chem. Soc.*, 2022, **144**, 6558–6565; (*e*) S. Guo, P. Cui, X. Liu and G. Jin, *J. Am. Chem. Soc.*, 2022, **144**, 22221–22228; (*f*) X. Liu, P. Cui, S. Guo, Y. Lin and G. Jin, *J. Am. Chem. Soc.*, 2023, **145**, 8569–8575; (*g*) X.-R. Liu, P.-F. Cui, Y. García-Rodeja, M. Solà and G.-X. Jin, *Chem. Sci.*, 2024, **15**, 9274–9280; (*h*) A. Saha, E. Oleshkevich, C. Vinas and F. Teixidor, *Adv. Mater.*, 2017, **29**, 1704238.

3 (*a*) R. Nunez, M. Tarrés, A. Ferrer-Ugalde, F. F. de Biani and F. Teixidor, *Chem. Rev.*, 2016, **116**, 14307–14378; (*b*) J. Ochi, K. Tanaka and Y. Chujo, *Angew. Chem., Int. Ed.*, 2020, **59**, 9841–9855; (*c*) Z. Wu, J. Nitsch, J. Schuster, A. Friedrich, K. Edkins, M. Loebnitz, F. Dinkelbach, V. F. Stepanenko, V. Würthner, C. M. Marian, L. Ji and T. B. Marder, *Angew. Chem., Int. Ed.*, 2020, **59**, 17137–17144; (*d*) L. Ji, S. Riese, A. Schmiedel, M. Holzapfel, M. Fest, J. Nitsch, B. F. E. Curchod, A. Friedrich, L. Wu, H. H. A. Mamari, S. Hammer, J. Pflaum, M. A. Fox, D. J. Tozer, M. Finze, C. Lambert and T. B. Marder, *Chem. Sci.*, 2022, **13**, 5205–5219; (*e*) D. K. You, H. So, C. H. Ryu, M. Kim and K. M. Lee, *Chem. Sci.*, 2021, **12**, 8411–8423; (*f*) X. Li, X. Tong, Y. Yin, H. Yan, C. Lu, W. Huang and Q. Zhao, *Chem. Sci.*, 2017, **8**, 5930–5940; (*g*) K. Yuhara and K. Tanaka, *Chem. Sci.*, 2025, **16**, 6495–6506; (*h*) F. Lerouge, A. Ferrer-Ugalde, C. Viñas, F. Teixidor, R. Sillanpää, A. Abreu, E. Xochitiotzi, N. Farfán, R. Santilland and R. Núñez, *Dalton Trans.*, 2011, **40**, 7541–7550.

4 (*a*) Y. Xu, Y. Yang, Y. Liu, Z. Li and H. Wang, *Nat. Catal.*, 2023, **6**, 16–22; (*b*) Z. Lu, P. Qiu, H. Zhai, G.-G. Zhang, X.-W. Chen, Z. Lu, Y. Wu and X. Chen, *Angew. Chem., Int. Ed.*, 2024, **63**, e202412401; (*c*) J. R. Riffle, C. L. Jowers, S. Luna, M. D. Smith and D. V. Peryshkov, *Chem. Sci.*, 2025, **16**, 15997–16003; (*d*) B. J. Eleazer, M. D. Smith, A. A. Popov and D. V. Peryshkov, *Chem. Sci.*, 2017, **8**, 5399–5407; (*e*) P. Coburger, J. Leitl, D. J. Scott, G. Hierlmeier, I. G. Shenderovich, E. Hey-Hawkins and R. Wolf, *Chem. Sci.*, 2021, **12**, 11225–11235; (*f*) M. Keener, M. Mattejat, S.-L. Zheng, G. Wu, T. W. Hayton and G. Ménard, *Chem. Sci.*, 2022, **13**, 3369–3374; (*g*) J. Wang, L. Xiang, X. Liu, A. Matler, Z. Lin and Q. Ye, *Chem. Sci.*, 2024, **15**, 4839–4845; (*h*) S. Bairagi, D. K. Patel, D. Chatterjee, M. Kučeráková, J. Macháček, T. Base, T. Pradeep and S. Ghosh, *Chem. Sci.*, 2025, **16**, 14127–14139; (*i*) J. Xu, S. Yao, V. Postils, E. Matito, C. Lorent and M. Driess, *Chem. Sci.*, 2025, **16**, 10826–10832.

5 (*a*) A. Marfavi, P. Kavianpour and L. M. Rendina, *Nat. Rev. Chem.*, 2022, **6**, 486–504; (*b*) R. J. Grams, W. L. Santos, I. R. Scorei, A. Abad-García, C. A. Rosenblum, A. Bita, H. Cerecetto, C. Viñas and M. A. Soriano-Ursua, *Chem. Rev.*, 2024, **124**, 2441–2511; (*c*) P. Stockmann, M. Gozzi, R. Kuhnert, M. B. Sárosi and E. Hey-Hawkins, *Chem. Soc. Rev.*, 2019, **48**, 3497–3512; (*d*) F. Issa, M. Kassiou and L. M. Rendina, *Chem. Rev.*, 2011, **111**, 5701–5722; (*e*) E. G. Tse, S. D. Houston, C. M. Williams, G. P. Savage, L. M. Rendina, I. Hallyburton, M. Anderson, R. Sharma, G. S. Walker, R. S. Obach and M. H. Todd, *J. Med. Chem.*, 2020, **63**, 11585–11601; (*f*) H. Li, Y. L. Gao and J. J. Ma, *Future Med. Chem.*, 2022, **14**, 1681–1692; (*g*) B. B. Jena and M. R. Pattanayak, *Carborane Clusters for Promoting Medicinal Applications*, Apple Academic Press: New Forms of Carbon, 2024, p. 219; (*h*) D. A. Gruzdev, G. L. Levit, V. P. Krasnov and V. N. Charushin, *Coord. Chem. Rev.*, 2021, **433**, 213753; (*i*) R. Otero, S. Seoane, R. Sigüeiro, A. Y. Belorusova, M. A. Maestro, R. Pérez-Fernández, N. Rochel and A. Mouriño, *Chem. Sci.*, 2016, **7**, 1033–1037; (*j*) W. Ma, Y. Wang, Y. Xue, M. Wang, C. Lu, W. Guo, Y.-H. Liu, D. Shu, G. Shao, Q. Xu, D. Tu and H. Yan, *Chem. Sci.*, 2024, **15**, 4019–4030; (*k*) M. Couto, M. F. García, C. Alamón, M. Cabrera, P. Cabral, A. Merlino, F. Teixidor, H. Cerecetto and C. Viñas, *Chem. – Eur. J.*, 2018, **24**, 3122–3126.

6 (*a*) Y. Wang, J. Nie, W. Fang, L. Yang, Q. Hu, Z. Wang, J. Z. Sun and B. Z. Tang, *Chem. Rev.*, 2020, **120**, 4534–4577; (*b*) F. Würthner, *Angew. Chem., Int. Ed.*, 2020, **59**, 14192–14196; (*c*) C. Chen, X. Zhang, Z. Gao, G. Feng and D. Ding, *Nat. Protoc.*, 2024, **19**, 2408–2434.

7 D. Ma, H. Bian, M. Gu, L. Wang, X. Chen and X. Peng, *Coord. Chem. Rev.*, 2024, **505**, 215677.

8 W. Zhang, Y. Huang, Y. Chen, E. Zhao, Y. Hong, S. Chen, J. W. Y. Lam, Y. Chen, J. Hou and B. Z. Tang, *ACS Appl. Mater. Interfaces*, 2019, **11**, 10567–10577.

9 (*a*) M. L. Beer, J. Lemon and J. F. Valliant, *J. Med. Chem.*, 2010, **53**, 8012–8020; (*b*) A. Buzharevski, S. Paskaš, M.-B. Sárosi, M. Laube, P. Lönnecke, W. Neumann, B. Murganić, S. Mijatović, D. Maksimović-Ivanić, J. Pietzsch and E. Hey-Hawkins, *Sci. Rep.*, 2020, **10**, 4827.

10 (*a*) T. L. Heying, J. W. Ager Jr., S. L. Clark, R. P. Alexander, S. Papetti, J. A. Reid and S. I. Trotz, *Inorg. Chem.*, 1963, **2**, 1097–1105; (*b*) L. I. Zakharkin, A. I. Kovderov and V. A. Ol'shevskaya, *Russ. Chem. Bull.*, 1986, **35**, 1260–1266; (*c*) Z. Qiu and Z. Xie, *Angew. Chem., Int. Ed.*, 2008, **47**, 6572–6575; (*d*) A. Sousa-Pedrares, C. Viñas and F. Teixidor, *Chem. Commun.*, 2010, **46**, 2998–3000; (*e*) F. Zheng, T.-F. Leung, K.-W. Chan, H. H. Y. Sung, I. D. Williams,

Z. Xie and G. Jia, *Chem. Commun.*, 2016, **52**, 10767–10770; (*f*) H. Ni, Z. Lu and Z. Xie, *Dalton Trans.*, 2022, **51**, 104–110.

11 (*a*) V. I. Bregadze, *Chem. Rev.*, 1992, **92**, 209–223; (*b*) D. Olid, R. Nunez, C. Vinas and F. Teixidor, *Chem. Soc. Rev.*, 2013, **42**, 3318–3336; (*c*) X. Zhang and H. Yan, *Coord. Chem. Rev.*, 2019, **378**, 466–482; (*d*) Z. Qiu and Z. Xie, *Acc. Chem. Res.*, 2021, **54**, 4065–4079; (*e*) M. Herberhold, H. Yan, W. Milius and B. Wrackmeyer, *Angew. Chem., Int. Ed.*, 1999, **38**, 3689–3691; (*f*) Z. Qiu, Y. Quan and Z. Xie, *J. Am. Chem. Soc.*, 2013, **135**, 12192–12195; (*g*) X. Zhang, H. Zheng, J. Li, F. Xu, J. Zhao and H. Yan, *J. Am. Chem. Soc.*, 2017, **139**, 14511–14517; (*h*) Y. Baek, K. Cheong, G. H. Ko, G. U. Han, S. H. Han, D. K. Kim, D. Lee and P. H. Lee, *J. Am. Chem. Soc.*, 2020, **142**, 9890–9895; (*i*) H. A. Mills, J. L. Martin, A. L. Rheingold and A. M. Spokoyny, *J. Am. Chem. Soc.*, 2020, **142**, 4586–4591; (*j*) Z. Wang, J. Yu, J. Zhang, D. Zhang, Z. Qiu and Z. Xie, *Chem. Sci.*, 2025, **16**, 3705–3712; (*k*) H.-J. Cao, X. Wei, F. Sun, X. Zhang, C. Lu and H. Yan, *Chem. Sci.*, 2021, **12**, 15563–15571; (*l*) Y.-N. Ma, Y. Gao, Y. Ma, Y. Wang, H. Ren and X. Chen, *J. Am. Chem. Soc.*, 2022, **144**, 8371–8378; (*m*) Y. Ma, H. Ren, Y. Wu, N. Li, F. Chen and X. Chen, *J. Am. Chem. Soc.*, 2023, **145**, 7331–7342; (*n*) M. Hamdaoui, F. Liu, Y. Cornaton, X. Lu, X. Shi, H. Zhang, J. Liu, B. Spingler, J. Djukic and S. Duttwyler, *J. Am. Chem. Soc.*, 2022, **144**, 18359–18374; (*o*) W. Sun, Y. Jin, Y. Wang, Z. Wen, J. Sun, J. Yao, S. Duttwyler and H. Li, *Chem. Sci.*, 2025, **16**, 5942–5947; (*p*) H.-J. Cao, J.-X. Li, J.-H. Yan, M.-X. Liu, Q. Zhao, J. Zhang, J. Zhang and H. Yan, *Chem. Sci.*, 2025, **16**, 9406–9412; (*q*) X. Zhang and H. Yan, *Chem. Sci.*, 2018, **9**, 3964–3969; (*r*) H. Yang, Y. Guo, K. Cao, Q. Jiang, C. Teng, D. Zhu and S. Wang, *Chem. Commun.*, 2024, **60**, 1124–1127; (*s*) Y.-H. Liang, J.-X. Kang, Y. Wang, Y.-G. Li, H.-J. Cao, Q. Zhao, X. Chen and Y.-N. Ma, *Chem*, 2026, **12**, 102788; (*t*) Y.-F. Liang, L. Yang, B. B. Jei, R. Kuniyil and L. Ackermann, *Chem. Sci.*, 2020, **11**, 10764–10769; (*u*) L. Yang, B. B. Jei, A. Scheremetjew, B. Yuan, A. C. Stückl and L. Ackermann, *Chem. Sci.*, 2021, **12**, 12971–12976; (*v*) M. Zhu, P. Wang, Z. Wu, Y. Zhong, L. Su, Y. Xin, A. M. Spokoyny, C. Zou and X. Mu, *Chem. Sci.*, 2024, **15**, 10392–10401; (*w*) C. Tang and Z. Xie, *Angew. Chem., Int. Ed.*, 2015, **54**, 7662–7665; (*x*) J.-Y. Lu, H. Wan, J. Zhang, Z. Wang, Y. Li, Y. Du, C. Li, Z.-T. Liu, Z.-W. Liu and J. Lu, *Chem. – Eur. J.*, 2016, **22**, 17542–17546; (*y*) R. M. Dziedzic and A. M. Spokoyny, *Chem. Commun.*, 2019, **55**, 430–442; (*z*) M. Gazvoda, H. H. Dhanjee, J. Rodriguez, J. S. Brown, C. E. Farquhar, N. L. Truex, A. Loas, S. L. Buchwald and B. L. Pentelute, *J. Am. Chem. Soc.*, 2022, **144**, 7852–7860.

12 (*a*) Q. Song, J. Yang, K. Zheng, T. Zhang, C. Yuan, L.-M. Yuan and X. Hou, *J. Am. Chem. Soc.*, 2024, **146**, 7594–7604; (*b*) Q. Zhao, H. J. Qi and T. Xie, *Prog. Polym. Sci.*, 2015, **49–50**, 79–120.

13 (*a*) M. Sun, L. Feng and J.-Y. Lu, *Org. Lett.*, 2024, **26**, 3697–3702; (*b*) W. R. Gill, P. L. Herbertson, J. A. H. MacBride and K. Wade, *J. Organomet. Chem.*, 1996, **507**, 249–255.

14 J.-M. Gao, L. Wang, H.-J. Yu, A.-G. Xiao and W.-B. Ding, *Pyrotechnics*, 2011, **36**, 404–409.

15 (*a*) D. Tu, P. Leong, S. Guo, H. Yan, C. Lu and Q. Zhao, *Angew. Chem., Int. Ed.*, 2017, **56**, 11370–11374; (*b*) X. Wei, M.-J. Zhu, Z. Cheng, M. Lee, H. Yan, C. Lu and J. Xu, *Angew. Chem., Int. Ed.*, 2019, **58**, 3162–3166.

16 J. Zhong, W. Zhu, S. Shen, N. Zhou, M. Xi, K. Du, D. Wang and B. Z. Tang, *Aggregate*, 2025, **6**, e70089.

17 J. Liu, H. Zhang, L. Hu, J. Wang, J. W. Y. Lam, L. Blancafort and B. Z. Tang, *J. Am. Chem. Soc.*, 2022, **144**, 7901–7910.

18 J. Mei, N. L. C. Leung, R. T. K. Kwok, J. W. Y. Lam and B. Z. Tang, *Chem. Rev.*, 2015, **115**, 11718–11940.

19 R. Coult, M. A. Fox, W. R. Gill, P. L. Herbertson, J. A. H. MacBride and K. Wade, *J. Organomet. Chem.*, 1993, **462**, 19–29.

20 Y. Hisata, D. Morishita and Y. Hoshimoto, *J. Am. Chem. Soc.*, 2025, **147**, 37677–37687.

21 M. J. Strauss, K. X. Liu, M. E. Greaves, J. C. Dahl, S.-T. Kim, Y.-J. Wu, M. A. Schmidt, P. M. Scola and S. L. Buchwald, *J. Am. Chem. Soc.*, 2024, **146**, 18616–18625.

22 (*a*) CCDC 2496931: Experimental Crystal Structure Determination, 2026, DOI: 10.5517/ccdc.csd.cc2pt85z; (*b*) CCDC 2496932: Experimental Crystal Structure Determination, 2026, DOI: 10.5517/ccdc.csd.cc2pt860; (*c*) CCDC 2496933: Experimental Crystal Structure Determination, 2026, DOI: 10.5517/ccdc.csd.cc2pt871; (*d*) CCDC 2496934: Experimental Crystal Structure Determination, 2026, DOI: 10.5517/ccdc.csd.cc2pt882; (*e*) CCDC 2496936: Experimental Crystal Structure Determination, 2026, DOI: 10.5517/ccdc.csd.cc2pt8b4.